

# The Mechanics of Fine Manipulation by Pushing

Kevin M. Lynch

The Robotics Institute  
Carnegie Mellon University  
Pittsburgh, PA 15213  
lynch@ri.cmu.edu

## Abstract

This paper presents a method for determining the possible instantaneous motions of a sliding object during multiple contact pushing. The approach consists of two components: a kinematic analysis considering kinematic motion constraints, and a force analysis considering force constraints on the motion. A new representation of the support friction of a sliding object is presented, and the results of the force analysis are independent of the exact support distribution of the object. The analysis results in a new manipulation primitive: stable rotational pushing. This primitive may be used for precise placement operations by pushing.

## 1. Introduction

One well-known approach to the problem of repositioning an object is pick-and-place: grasp the object, carry it to the new location, and disengage it. As Mason [12] notes, however, pushing the object may be preferable if the initial and goal locations share the same support surface. This avoids the difficulties involved in grasping and releasing the object and provides a solution for manipulators lacking the dexterity, size, and strength necessary to grasp and lift the object. The ability to precisely position objects by pushing can greatly extend a robot's manipulation capability.

Consider the example shown in figure 1. The rectangular block is pushed (perhaps by a mobile robot) to the final location by edge-edge contact. In order to plan a pushing operation like this, two questions must be answered: 1) What directions can the object be pushed while maintaining stable contact? and 2) How should these motion constraints be used to plan a pushing trajectory (possibly considering obstacles)?

In this paper we will develop the analytical tools to answer the first question. We pose the pushing problem more generally than it previously has been: Given multiple point contacts and an arbitrary pusher motion, what is the set of all possible motions of the sliding object? The answer to this question provides the next step toward making pushing a more useful robotic capability. Previous work on pushing has resulted in an increased repertoire of robot actions, including stable translational pushing of sliding objects [1, 2, 4, 5, 11, 15]. The analysis presented here allows us to extend the class of stable motions of a pushed sliding object to include rotations as well as translations. This new robot primitive may be used to execute precise *planar parts transfer* tasks. Other applications of the analysis will also be discussed.

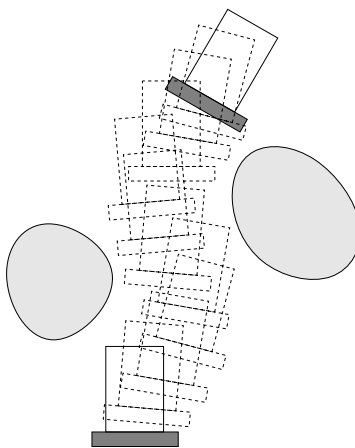


Figure 1: A pushing trajectory to move the object from the initial to goal location.

### 1.1. Definitions

The *slider* is manipulated by a *pusher*. The slider and pusher may each consist of multiple rigidly attached rigid bodies. The *contact configuration* specifies the kinematic constraints imposed on the slider by the pusher. In this paper, all contact configurations may be reduced to a finite set of contact points (see figure 2). The *contact mode* is given by the instantaneous motion of these contacts. Each contact point receives one of four possible labels indicating the motion of the slider relative to the pusher at the contact point: **s** (sticking) if there is no relative motion, **r** (right-sliding), **l** (left-sliding), and **f** (breaking free) if the contact is broken. The contact mode is denoted by the concatenation of the individual contact labels (see figure 3).

Friction forces are governed by *Coulomb's Law*. At any contact,  $f_t \leq \mu f_n$ , where  $f_t$  is the tangential (frictional) force,  $f_n$  is the normal force, and  $\mu$  is the *coefficient of friction*. (For ease of discussion, we will assume the *static* and *dynamic* coefficients of friction are equal, although this is not strictly necessary.) At a sticking contact, the force may lie anywhere within the *friction cone*. At a sliding contact, the total force felt by an object lies on the edge of the friction cone opposite the motion of the object relative to the contacted surface.

Planar velocities will be described as an instantaneous rotation about a *center of rotation* (COR) in the plane. We are not concerned with velocity magnitudes in this paper; frictional forces under Coulomb's Law depend only on the direction of contact motion, not its rate. Therefore, a velocity is completely

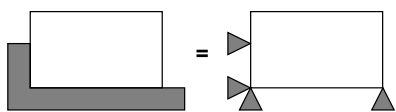


Figure 2: Equivalent contact configurations.

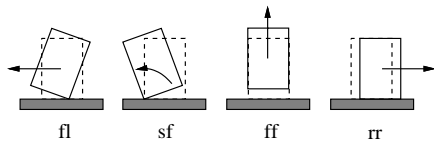


Figure 3: Four contact modes for initial edge-edge contact.

specified by the two coordinates of the COR and the sign of rotation (clockwise [-] or counterclockwise [+]). This is called a *signed COR*. Translational motions correspond to CORs at infinity.

The motion of the pusher is given by a signed  $COR_p$ ; the slider motion is a signed  $COR_s$ .

## 1.2. Previous work

Mason was the first to analyze the friction mechanics of planar sliding in the context of robotics [15]. One elegant result of his analysis is a simple rule for determining the rotation sense of a slider in contact with a point pusher, using only the location of the slider center of mass, the contact point and normal, the push direction, and the coefficient of friction between the pusher and slider. Peshkin and Sanderson [16] extended Mason's work by determining bounds on the set of possible CORs. Goyal [8] developed a three-dimensional *limit surface* in force-moment space describing the relationship between the motion of a slider and the total frictional support force.

Mason's results have been used to find stable translational pushes [1, 2, 4, 5, 11, 15] and guaranteed successful parallel-jaw grasping strategies [4, 7] despite uncertainty in object location and physical parameters. Peshkin and Sanderson applied their results to planning a sequence of fences suspended over a conveyor belt to eliminate position and orientation uncertainty of a workpiece [17].

The style of analysis adopted in this paper is similar to that used by Brock [3] and Mason [13]. In [3] the kinematically possible motions of a grasped object are determined, and then a force is applied to the object to cause it to slip in the grasp in a desired manner. In order to synthesize a robot motion to push a block along a wall, Mason [13] first finds the possible contact modes and the implied frictional forces at the block-wall interface and the wall-support interface. Using this information, a pushing motion and contact is chosen such that the pushing force can only be balanced by the contact mode corresponding to the block sliding along the wall.

## 1.3. Problem statement

Given:

1. the geometry of a rigid planar slider on a horizontal support plane,
2. the slider center of mass,
3. the pusher-slider contact configuration,
4. the coefficient of friction between the pusher and slider, and

## 5. the pusher motion $COR_p$ ,

find all possible instantaneous slider motions.

This paper builds primarily on the work of Mason and Peshkin. Whereas they considered the motion of a slider in point contact with a pusher, this work finds all possible motions of a slider given a pusher with an arbitrary motion and multiple point contacts. Using this information, we can find the set of pusher motions which maintain the pusher-slider contact configuration. These motions may be continued indefinitely and can be used for planar parts transfer operations. This type of push may be termed a *stable non-grasp*; all possible frictional support forces can be balanced by the pushing contact forces and stable contact is guaranteed. We will briefly discuss the synthesis of stable non-grasps.

Another application of the results of this paper is finding pusher motions resulting in a unique slider contact mode other than stable contact. This may be used to reduce uncertainty in the slider position. As an example, consider a block in edge-edge contact with a pusher. If we push at a sharp angle with low contact friction, the block is guaranteed to slide along the pusher, perhaps until it reaches a point where stable contact is guaranteed (i.e., a mechanical stop).

## 1.4. Assumptions

1. Motions are slow enough that inertial forces are negligible. This is the *quasi-static* assumption; frictional forces only are considered.
2. All motions and forces are in a plane normal to the gravity vector.
3. Friction forces conform to Coulomb's Law.
4. The coefficient of friction is uniform between the slider and support surface.

## 1.5. Approach

To solve the problem posed in section 1.3, we first perform a kinematic analysis to determine the set of kinematically possible  $COR_s$ . This procedure takes as input the pusher-slider contact configuration and the  $COR_p$  and returns a set of contact modes and the corresponding  $COR_s$  regions. For each contact mode, the next step is to determine the slider motions which are consistent with the implied contact forces. This set of *force possible*  $COR_s$  is then intersected with the set of kinematically possible  $COR_s$ . If the intersection is null, this contact mode cannot result. If the intersection is non-null, this contact mode may occur and any of the  $COR_s$  in the intersection could be the actual instantaneous slider motion. The set of all possible instantaneous slider motions is the union over all contact modes of the intersections of the kinematically and force possible  $COR_s$ . The approach is illustrated in figure 4.

## 2. Kinematic analysis

This section outlines the method for determining the kinematic constraints on the motion of the slider. First we employ Reuleaux' method to find the set of kinematically possible  $COR_s$  relative to the pusher. Given the  $COR_p$ , the legal motions are then mapped to a reference frame fixed in the support surface.

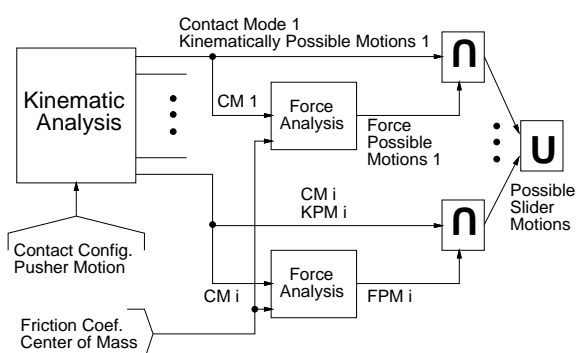


Figure 4: Solution method block diagram.

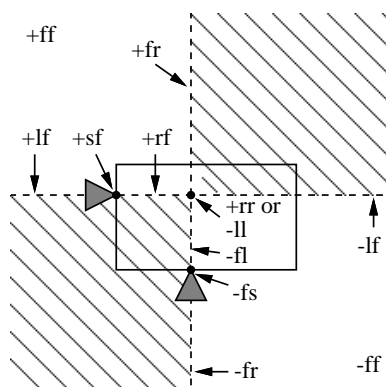


Figure 5: Kinematically legal CORs and contact modes. Hatched regions correspond to illegal CORs.

## 2.1. Reuleaux' method

Reuleaux [18] describes a method for determining the kinematically admissible instantaneous planar motions of a movable object in contact with a fixed object. Each contact normal divides the plane by the sense of legal rotation centers for the movable object. Any movable object COR must have a positive (counterclockwise) sense if it lies to the left of a contact normal and a negative (clockwise) sense if it lies to the right. A COR lying on the contact normal can have either rotation sense. Any signed COR consistent with all contact normal constraints is a kinematically legal motion.

The contact modes corresponding to the kinematically legal motions are easily found. For a particular contact, a COR at the contact point corresponds to sticking contact  $s$ . A COR at any other point on the contact normal corresponds to either right-sliding  $r$  or left-sliding  $l$ , depending on the sign of the COR. Any other valid COR results in breaking contact  $f$ . An example showing the full set of contact modes and corresponding  $COR_s$  regions is given in figure 5.

## 2.2. Combining velocities in COR space

If we consider the pusher to be the fixed object and the slider to be the movable object, Reuleaux' method finds the kinematically possible motions of the slider relative to the pusher. Our real goal, however, is to find the kinematically legal slider motions relative to a reference frame fixed in the support plane. The slider motion in this reference frame is a positive linear combination of

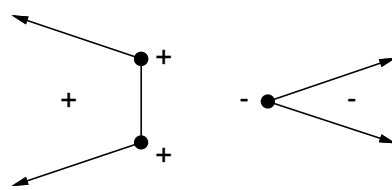


Figure 6: Positive linear combinations of instantaneous CORs.

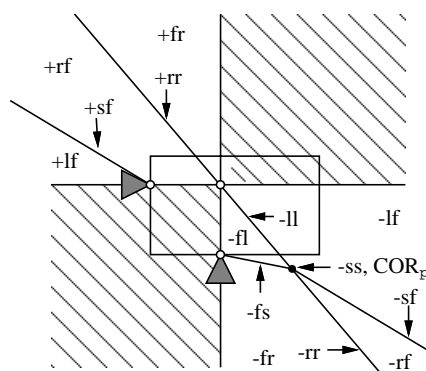


Figure 7: Kinematically legal  $COR_s$  (in a reference frame fixed in the support plane) and associated contact modes for a given  $COR_p$ . The  $COR_p$  is clockwise and all  $COR_s$  in the lower right quadrant are clockwise. All  $COR_s$  in the upper left quadrant are counterclockwise.

the pusher motion and the slider motion relative to the pusher.

The positive linear combination of two planar velocities represented by signed CORs has a simple graphical representation. If the two CORs have the same sign, a positive linear combination of these velocities corresponds to a COR of the same sign somewhere on the line segment connecting the two CORs. If the CORs are of opposite sign, the resulting COR must lie somewhere on the line connecting the two, but not between the two (i.e., on the *external* line segment). The sense of CORs on the external line segment changes at infinity, which corresponds to pure translation. See figure 6.

## 2.3. Admissible contact modes and slider motions

The entire space of kinematically legal slider velocities is found by applying Reuleaux' method and then incorporating the  $COR_p$  to map the set of legal  $COR_s$  to the support plane reference frame. Under this positive linear combination mapping, a single  $COR_s$  maps to a line segment, a line segment maps to a region, and a region maps to another region.<sup>1</sup> In general a signed  $COR_s$  and a signed  $COR_p$  do not completely disambiguate the contact mode, however; the relative angular velocities must be considered. A  $(COR_p, COR_s)$  pair may correspond to multiple contact modes.

Figure 7 illustrates the set of kinematically legal  $COR_s$  in the support plane reference frame for the contact configuration given in figure 5 and the clockwise (-)  $COR_p$  shown. The  $COR_s$  regions for the  $ff$  contact mode are never mapped, since this contact mode implies zero contact force and therefore zero slider motion (under the quasi-static assumption). In this example, because all

<sup>1</sup>This mapping is actually a *strictly positive* linear combination. Line segments are open-ended and regions do not include their boundaries.

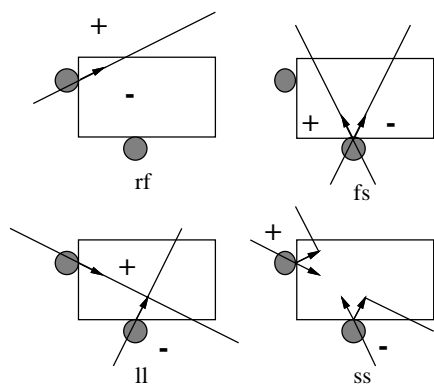


Figure 8: Moment-labeling representation of contact forces for various contact modes.

pushing contacts are moving into the slider, any  $(COR_p, COR_s)$  pair is either kinematically illegal or the contact mode and relative angular velocities can be uniquely determined. In other words, the  $COR_s$  regions for different contact modes do not overlap.<sup>2</sup> Also notice that if  $COR_s = COR_p$  the contact mode is **ss**. Finally, since the set of  $COR_s$  for any contact mode is a linear combination of the  $COR_p$  and the motions found by Reuleaux' method, the  $COR_s$  regions corresponding to all contact modes meet at the  $COR_p$ .

### 3. Force analysis

Under the quasi-static assumption, the slider frictional support force must always balance the pusher contact force. For each contact mode returned by the kinematic analysis, the set of possible contact forces is easily found. The force possible slider motions are those which correspond to a frictional support force that can be balanced by the possible contact forces.

#### 3.1. Pusher contact forces

The set of possible contact forces may be found directly from the contact mode and the coefficient of friction. At a **s** contact, the force acting on the slider may lie anywhere within the friction cone. The force acting on the slider at a **r** or **l** contact must lie on the left or right edge of the friction cone, respectively. No force may act at a contact point labeled **f**, as the contact is breaking at that point. The total contact force is a positive linear combination of the forces applied at each contact point.

Figure 8 shows the possible forces acting at each contact for four different contact modes. The resultant sets of forces are given by their *moment-labeling* regions [14]. Any applied force must make nonnegative moment about the + region and nonpositive moment about the - region. For the **ss** contact mode, the regions disappear for a friction coefficient greater than 1. In this case, the set of possible contact forces spans the force space.

#### 3.2. Frictional support forces

We will use the following notation to describe frictional support forces (from [15]):

<sup>2</sup>Note that it is possible for contact to be maintained at a pushing point with a motion component opposite the contact normal. This results in  $COR_s$  region overlap for different contact modes.

$R$	region of contact between the slider and support plane
$dA$	differential element of area of $R$
$\vec{x}$	position of $dA$
$p(\vec{x})$	pressure at $\vec{x}$ ( $p(\vec{x}) \geq 0$ for all $\vec{x}$ )
$\mu_s$	coefficient of friction between the slider and support
$\vec{f}$	frictional force vector
$m$	signed magnitude of the frictional moment

Locating the origin of the coordinate system at the  $COR_s$ , the total frictional force  $\vec{f}$  is given by

$$\vec{f} = -\mu_s \text{sgn}(\dot{\theta}) \hat{k} \times \int_R \frac{\vec{x}}{|\vec{x}|} p(\vec{x}) dA \quad (1)$$

where  $\hat{k}$  is the unit vector normal to the support plane and  $\dot{\theta}$  is the angular velocity about  $\hat{k}$ . The frictional moment about the  $COR_s$  is

$$m \hat{k} = -\mu_s \text{sgn}(\dot{\theta}) \hat{k} \int_R |\vec{x}| p(\vec{x}) dA \quad (2)$$

Mason showed that during slider translation, the frictional force directly opposes the motion and acts through the projection of the slider center of mass onto the support plane. This point is called the *center of friction*, or CF [15]. The frictional support force always acts through the CF for translational motions regardless of the form of the slider support pressure distribution  $p(\vec{x})$ . Thus, for the special case of translational motion, the support distribution reduces to a single point of support located at the CF.

##### 3.2.1. The effective center of friction

In this paper, we are interested in the frictional forces during general slider motion, which includes rotation. Therefore we will define the *effective center of friction*, or  $CF_{eff}$ . The  $CF_{eff}$  for an arbitrary instantaneous motion plays an analogous role to the CF for translations. For a known  $COR_s$  and  $p(\vec{x})$ , the support distribution may be treated as a single point at the  $CF_{eff}$ .

To find the vector from the  $COR_s$  to the  $CF_{eff}$  (denoted  $\vec{c}$ ), we first observe that the vector  $\vec{d}$  in the direction of  $\vec{c}$  ( $\vec{d}/|\vec{d}| = \vec{c}/|\vec{c}|$ ) is perpendicular to  $\vec{f}$  and is given by  $\text{sgn}(\dot{\theta}) \hat{k} \times \vec{f}$ , or

$$\vec{d} = \mu_s \int_R \frac{\vec{x}}{|\vec{x}|} p(\vec{x}) dA \quad (3)$$

The magnitude of the moment is

$$|m| = \mu_s \int_R |\vec{x}| p(\vec{x}) dA \quad (4)$$

Noting that the magnitude of the frictional force is  $|\vec{d}|$ , we find the length of the vector  $\vec{c}$ :

$$|\vec{c}| = \frac{|m|}{|\vec{d}|} \quad (5)$$

Combining the direction and magnitude information from equations 3 and 5, the vector from the  $COR_s$  to the  $CF_{eff}$  is given by

$$\vec{c} = \frac{|m|}{|\vec{d}|^2} \vec{d} \quad (6)$$

The distance from the  $COR_s$  to the  $CF_{eff}$  is always greater than or equal to the distance from the  $COR_s$  to the CF. Unlike the CF, the  $CF_{eff}$  is not constrained to lie within the convex hull of  $R$ . Note also that  $\vec{c}$  does not depend on  $\mu_s$  or the sense of the  $COR_s$ .

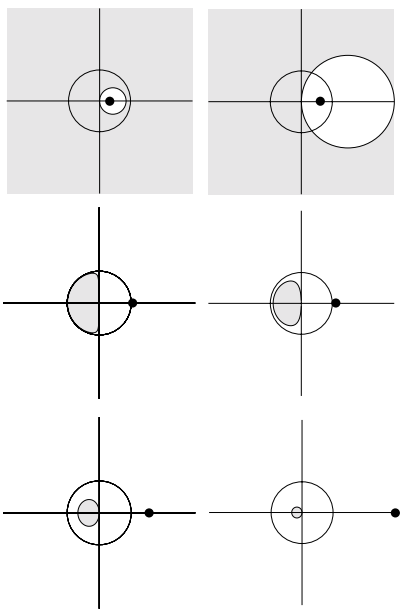


Figure 9:  $\{CF_{eff}\}$  (shaded) as the  $COR_s$  moves out along a ray.

### 3.2.2. Indeterminacy of $p(\vec{x})$

If we can evaluate equation 6 for a given signed  $COR_s$ , the slider motion and the frictional support force are completely described by the  $COR_s$  and the  $CF_{eff}$ . Unfortunately, equation 6 depends on the exact form of  $p(\vec{x})$ , which is generally not available as it depends on the microscopic interaction of the slider and support surface. We would like to find the set of  $CF_{eff}$  resulting from any possible  $p(\vec{x})$  consistent with the known CF. This set, denoted  $\{CF_{eff}\}$ , is guaranteed to contain the actual  $CF_{eff}$ . In other words, due to the unknown  $p(\vec{x})$ , we cannot find the exact frictional support force, but a set known to contain the actual force.

In order to find the  $\{CF_{eff}\}$  for a given  $COR_s$ , we use the simplification adopted by Peshkin and Sanderson. (See [16] for details.) The support region of the slider is modeled as the smallest disk centered at the CF which contains the entire contact region  $R$ . The disk model is a conservative approximation, as the  $\{CF_{eff}\}$  for the disk must be a superset of the  $\{CF_{eff}\}$  for the slider. Tighter bounds on the  $\{CF_{eff}\}$  may be obtained, but we will not address this issue here.

There is a simple closed-form expression for the  $\{CF_{eff}\}$  and its moment-labeling representation for the case of a  $COR_s$  inside the disk. For a  $COR_s$  outside the disk, the  $\{CF_{eff}\}$  and moment-labeling representation may be found parametrically (see [10] for details). Figure 9 shows the  $\{CF_{eff}\}$  as the  $COR_s$  moves out along a ray from the CF. For a given  $COR_s$ , the slider support must reduce to a single point somewhere in the  $\{CF_{eff}\}$ . The intersection of the axes is the slider CF, and the slider may be any shape within the disk. These figures may be rotated to obtain the  $\{CF_{eff}\}$  for  $COR_s$  along any other ray.

It is important to note that the  $\{CF_{eff}\}$  shrinks as the  $COR_s$  moves out along a ray from the CF. This implies that the set of possible frictional support forces also shrinks. For a  $COR_s$  near the CF, the  $CF_{eff}$  may lie almost anywhere in the plane. For a  $COR_s$  at infinity, the  $\{CF_{eff}\}$  becomes a single point at the slider CF. This is consistent with the fact that the support distribution can be reduced to a single point at the CF for slider translations.

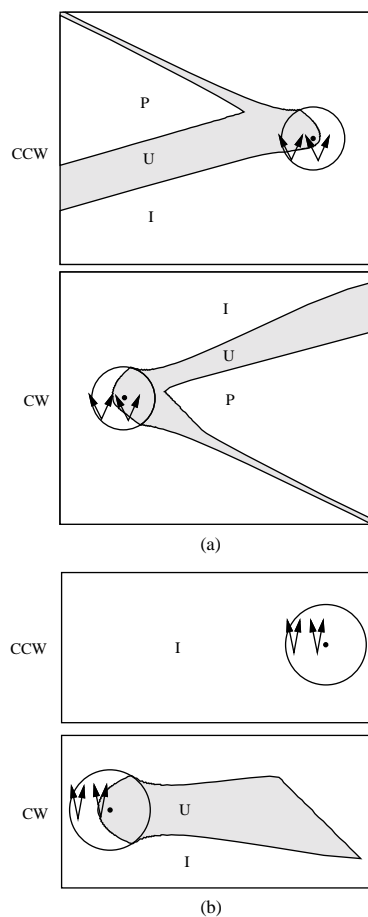


Figure 10: Force status of all motions for two example contact modes.

### 3.3. Slider motion force status

We would like to know if a given  $COR_s$  is force possible for a particular contact mode. To answer this question, we must determine if the set of possible frictional support forces for this  $COR_s$  is balanced by the set of possible contact forces. The result is the *force status* of the  $COR_s$ , which must be one of the following three:

- I None of the possible frictional support forces can be balanced by the set of possible contact forces. This  $COR_s$  is force **Impossible**. This slider motion cannot occur for the given contact mode.
- U Some, but not all, of the possible frictional support forces can be balanced by the set of possible contact forces. This  $COR_s$  may or may not be force possible, depending on  $p(\vec{x})$ . The  $COR_s$  status is **Undetermined**.
- P All of the possible frictional support forces can be balanced by the set of possible contact forces. This  $COR_s$  is force **Possible**.

The status of a  $COR_s$  may be determined using geometric intersection in the moment-labeling representation.

### 3.4. Force status for all motions

If  $p(\vec{x})$  is known, we may construct the slider limit surface [8] in three-dimensional force-moment space. The limit surface completely characterizes the relationship between the motion and frictional support force. The frictional load lies on the limit surface during quasi-static motion, and the direction of the slider motion is normal to the surface in three-dimensional velocity space (two translational components and one angular component). Thus, for a particular contact mode, if we construct the convex hull of the pusher-slider contact forces in force-moment space [6] and project it to the limit surface, the set of normals to the intersected surface are the slider motions which are labeled P. All other slider motions are labeled I.

This method of determining the force status of slider motions is impractical, as it assumes a known  $p(\vec{x})$ . Instead, we can use the weaker model of a known slider CF and bounding disk. One price of using this weaker model, as we have already seen, is that some motions will be labeled U.

In section 3.2.2 we observed that as the signed  $COR_s$  moves out along a ray from the CF to infinity, the set of possible frictional support forces shrinks. This enables the use of binary search to find the force status of all  $COR_s$  of the same rotation sense along a particular ray. A signed  $COR_s$  moving along a ray from the CF to infinity must either:

1. always be labeled I,
2. transition from U to I,
3. always be labeled P<sup>3</sup>, or
4. transition from U to P.

Any translation ( $COR_s$  at infinity) is either labeled I or P, since the  $\{CF_{eff}\}$  reduces to a single point at the CF, implying a single possible frictional support force.

The strategy for finding the force status of all slider motions is to sample rays at angles from 0 to  $2\pi$  and binary search for the transition in force status, if there is one, along each ray. Each ray should be searched twice, once for each rotation sense. Adjoining ray segments with the same label are then merged into regions.

Figure 10 shows two examples of this procedure. In 10(a), there are two sticking contacts with parallel contact normals and contact friction  $\mu_c = 0.5$ . The force possible, impossible, and undetermined slider motions are represented in two diagrams, one for the plane of counterclockwise  $COR_s$  and one for the plane of clockwise  $COR_s$ . If the exact  $p(\vec{x})$  of the slider were known, the U region would disappear and the boundary between the P and I region would lie within the U region shown.

10(b) again shows two sticking contacts with parallel contact normals and  $\mu_c = 0.2$ . In this example, however, there is no P region. Since no contact force can pass through the CF, translation of the slider is impossible. This means that all  $COR_s$  at infinity are labeled I; therefore, no  $COR$  will be labeled P. In fact, since any possible contact force must pass to the left of the CF, the slider can only rotate clockwise.

If the set of possible contact forces is a single line of force, the procedure described here will simply return the  $COR$  locus found in [16]. The  $COR$  locus is a single region labeled U. The U region in 10(b) is equivalent to the union of the  $COR$  loci for all lines of force between the two contacts and inside the friction cone.

<sup>3</sup>This only occurs when the set of possible contact forces spans the force space. In this case, all  $COR_s$  are labeled P.

## 4. Combined analysis

As described in section 1.5, the force P and U  $COR_s$  regions for each contact mode are intersected with the corresponding kinematically possible  $COR_s$  regions. If we do this for all contact modes, the resulting intersection sets are guaranteed to contain the actual instantaneous  $COR_s$ .

The results of the analysis are most useful when only a single contact mode can result, despite uncertainty in  $p(\vec{x})$ . When this contact mode is sticking at all contact points, the push is called *stable*; the contact configuration is maintained and the push may be continued indefinitely. Examples will be given in the next section.

## 5. Examples and experiment

### 5.1. Example 1: Stable pushing

A useful application of the preceding analysis is the identification of the set of stable pushing operations for a given contact configuration. In this example, the slider is a 9V battery lying on its side. The pusher is a straight edge in aligned edge-edge contact with the face of the battery opposite the terminals, and the coefficient of friction between the pusher and slider is 1.0.

Because we are interested in finding the set of all stable  $COR_p$ , and not just the possible motions for a particular  $COR_p$ , we defer the kinematic analysis until later. Instead, we simply enumerate the possible contact modes using Reuleaux' method and find the corresponding force P, U, and I  $COR_s$  regions. Any guaranteed stable  $COR_p$  must lie in the P region of the *ss* contact mode. The set of guaranteed stable pushes is all  $COR_p$  in this P region for which *ss* is the only possible contact mode.

For this example, all  $COR_p$  in the *ss* P region are guaranteed to be stable. The full proof cannot be given here for space reasons, but figure 11 gives an example for a clockwise  $COR_p$  chosen in the *ss* P region. 11(a) shows the kinematically possible motions and contact modes. Figure 11(b) shows the clockwise P and U  $COR_s$  regions for *ss* contact. By symmetry, the counterclockwise regions are just a mirror image of these regions about a vertical line through the CF. For two sample contact modes, *fr* (figure 11(c)) and *sf* (figure 11(d)), the kinematically possible and force U  $COR_s$  regions do not intersect. In fact, this is the case for all contact modes other than *ss* for any choice of  $COR_p$  in the *ss* P region. Once edge-edge contact has been established, then, the slider will remain in stable contact as the pusher rotates about any point in the *ss* P region. Complex stable pushing operations may be executed by continuously changing the  $COR_p$  during the course of the push (as in figure 1), provided the  $COR_p$  always remains inside the *ss* P region. Note that the force regions are drawn relative to the slider; they move with the slider during its motion.

#### One-step planning

Planning one-step pushing operations about a constant  $COR_p$  is straightforward. Given initial and goal positions and orientations, we simply find the  $COR_{total}$  corresponding to the total motion. If the  $COR_{total}$  is a guaranteed stable  $COR_p$ , the pusher motion given by  $COR_p = COR_{total}$  will achieve the goal.

Figure 12 shows an initial configuration of the battery and three goal configurations. Goal1 is guaranteed achievable by a one-step pushing plan, since the  $COR_{total}$  corresponding to the total motion lies inside the stable  $COR_p$  region. Goal3 is definitely not attainable by a one-step push. Goal2 may or may not be reachable by pushing about a constant  $COR_p$ .

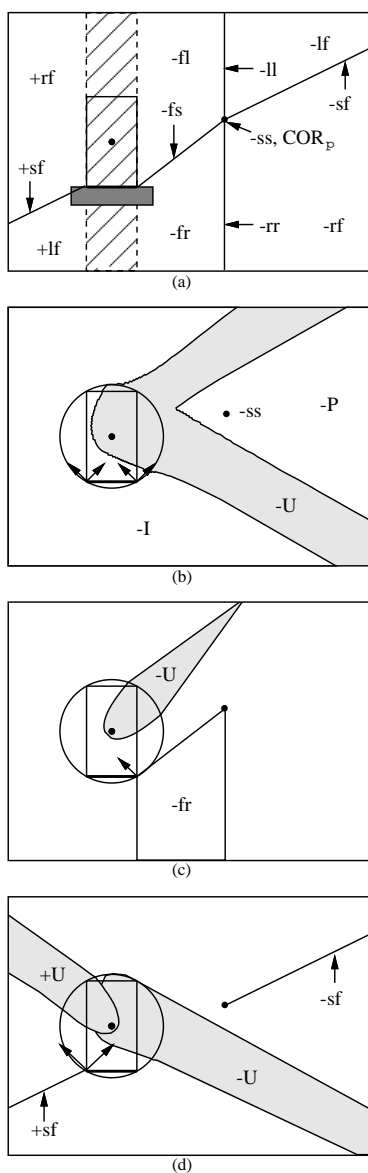


Figure 11: Clockwise  $COR_p$  is a guaranteed stable push.

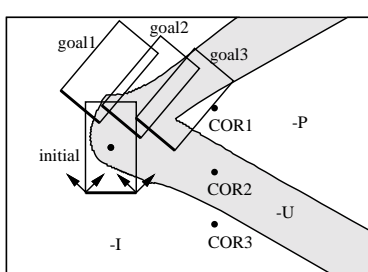


Figure 12: Clockwise CORs for three different goals.

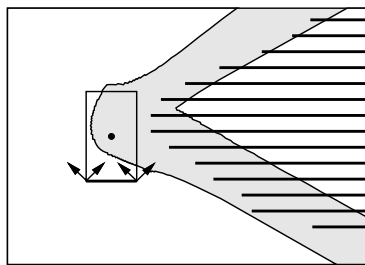


Figure 13: Experimentally stable clockwise  $COR_p$ .

### Experiment

In order to verify the validity of the physical assumptions, we experimentally determined the stable  $COR_p$  for the battery with  $\mu_c$  measured to be approximately 1.0. The experimental setup consists of a turntable with a fence suspended over it. By placing the battery in edge-edge contact with the fence and rotating the turntable, the same relative motion is created as slowly rotating the pusher about a  $COR_p$  at the turntable axis. By changing the  $x$  position of the battery on the fence and the  $y$  position of the fence, the effective  $x$  and  $y$  position of the  $COR_p$  is changed.

In this experiment, only the clockwise stable region is tested. The dark lines superimposed on the analytical results represent the experimentally stable  $COR_p$  (figure 13). For  $COR_p$  at these locations, the observed contact mode was *ss*. These results agree with the analysis. We expect the lines of stable  $COR_p$  to cover the *P* region but not reach into the *I* region. This is precisely the case. It should be noted, however, that small disturbance forces applied to the slider are sufficient to make  $COR_p$  near the boundary of the *P* region unstable.

### 5.2. Example 2: Contact synthesis

In the last example we found all stable motions for a particular contact configuration. Here we look at the inverse problem: Given a desired stable slider motion, how should the pusher contact the slider?

To simplify the problem, we will only consider the case of a fence pusher and a polygonal slider. The only possible stable contact configuration is edge-edge contact. For each slider edge we can calculate the region of guaranteed stable  $COR_p$  as in example 1. Given a desired slider motion, the robot would use the contact configuration which contains this motion in its guaranteed stable  $COR_p$  region.

Figure 14 shows the force *P* regions (which are also guaranteed stable  $COR_p$ ) for the given polygon and  $\mu_c = 0.5$ . The edges are numbered 1 to 4, starting with the horizontal edge and proceeding counterclockwise. The regions labeled *P*1–*P*4 are the guaranteed stable  $COR_p$  regions for edge-edge contact with edge 1–4, respectively. The *I* regions represent force impossible motions regardless of the contact edge. This information could be used to determine impossible slider trajectories for a pushing control system [9].

## 6. Extensions

For general planar parts transfer, the planning of sequences of stable pushes (or smoothly varying paths) is necessary. As shown in section 5.1, one-step planning is trivial. In the case where a one-step plan is either not stable for any contact configuration or causes a collision between the slider and an

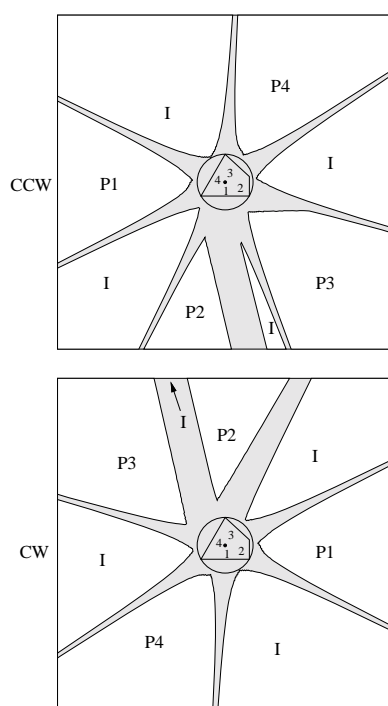


Figure 14: All possible and impossible slider motions for edge-edge pushing contact.

obstacle, a path planner incorporating the nonholonomic stable motion constraints is required. It can be shown that if a particular contact configuration has at least two stable non-translational  $COR_p$ , the slider may be positioned and oriented arbitrarily in the (obstacle-free) plane by pushing with this contact configuration.

This paper assumes a known pusher-slider contact configuration. Due to sensing and control errors, however, it is difficult for a robot to accurately achieve a particular contact configuration. One solution is to use the mechanics of pushing to decrease uncertainty in the contact configuration. For example, a fence pusher may translate until a slider edge aligns with the fence before executing a stable push.

To ensure analytical results which are robust in the real world, the analysis should allow for some uncertainty in physical parameters such as the coefficient of contact friction and the location of the CF. The effect of this uncertainty is to enlarge the force  $U$  regions.

The instantaneous analysis presented here could be coupled with an integration procedure and the  $c$ -space obstacle representing all possible pusher-slider contact configurations, as in [5]. This would allow us to reason about finite slider motions, and, in particular, to determine whether a slider perturbed from a stable push would tend to return to the original configuration.

## Acknowledgments

I would like to thank my advisors Matt Mason and Tom Mitchell for their support, and the members of the CMU Manipulation Lab, especially Matt Mason and (former member) Randy Brost, for many interesting discussions and helpful comments. This research was supported by NASA Ames Grant NCC 2-713.

## References

- [1] S. Akella and M. T. Mason. Posing polygonal objects in the plane by pushing. In *IEEE International Conference on Robotics and Automation*, pages 2255–2262, 1992.
- [2] Z. Balorda. Reducing uncertainty of objects by robot pushing. In *IEEE International Conference on Robotics and Automation*, pages 1051–1056, 1990.
- [3] D. L. Brock. Enhancing the dexterity of a robot hand using controlled slip. Master's thesis, Massachusetts Institute of Technology, 1987.
- [4] R. C. Brost. Automatic grasp planning in the presence of uncertainty. *International Journal of Robotics Research*, 7(1):3–17, Feb. 1988.
- [5] R. C. Brost. *Analysis and Planning of Planar Manipulation Tasks*. PhD thesis, Carnegie Mellon University, School of Computer Science, Jan. 1991.
- [6] M. A. Erdmann. On motion planning with uncertainty. Master's thesis, Massachusetts Institute of Technology, Aug. 1984.
- [7] K. Y. Goldberg. *Stochastic Plans for Robotic Manipulation*. PhD thesis, Carnegie Mellon University, School of Computer Science, Aug. 1990.
- [8] S. Goyal. *Planar Sliding of a Rigid Body With Dry Friction: Limit Surfaces and Dynamics of Motion*. PhD thesis, Cornell University, Dept. of Mechanical Engineering, 1989.
- [9] M. Inaba and H. Inoue. Vision-based robot programming. In *International Symposium on Robotics Research*, 1989.
- [10] K. M. Lynch. The mechanics of fine manipulation by pushing. Forthcoming Robotics Institute Technical Report.
- [11] M. Mani and W. Wilson. A programmable orienting system for flat parts. In *NAMRI XIII*, 1985.
- [12] M. T. Mason. Mechanics and planning of manipulator pushing operations. *International Journal of Robotics Research*, 5(3):53–71, Fall 1986.
- [13] M. T. Mason. Compliant sliding of a block along a wall. In *International Symposium on Experimental Robotics*, June 1989.
- [14] M. T. Mason. Two graphical methods for planar contact problems. In *IEEE/RSJ International Conference on Intelligent Robots and Systems*, Nov. 1991.
- [15] M. T. Mason and J. K. Salisbury, Jr. *Robot Hands and the Mechanics of Manipulation*. The MIT Press, 1985.
- [16] M. A. Peshkin and A. C. Sanderson. The motion of a pushed, sliding workpiece. *IEEE Journal of Robotics and Automation*, 4(6):569–598, Dec. 1988.
- [17] M. A. Peshkin and A. C. Sanderson. Planning robotic manipulation strategies for workpieces that slide. *IEEE Journal of Robotics and Automation*, 4(5):524–531, Oct. 1988.
- [18] F. Reuleaux. *The Kinematics of Machinery*. MacMillan, 1876. Reprinted by Dover, 1963.